Multi-unit recordings reveal context-dependent modulation of synchrony in odor-specific neural ensembles

Thomas A. Christensen, Vincent M. Pawlowski, Hong Lei and John G. Hildebrand

Arizona Research Laboratories, Division of Neurobiology, University of Arizona, PO Box 210077, Tucson, Arizona 85721-0077, USA
Correspondence should be addressed to T.A.C. (tc@neurobio.arizona.edu)

We used neural ensemble recording to examine odor-evoked ensemble patterns in the moth antennal (olfactory) lobe. Different odors are thought to evoke unique spatiotemporal patterns of glomerular activity, but little is known about the population dynamics underlying formation of these patterns. Using a silicon multielectrode array, we observed dynamic network interactions within and between glomeruli. Whereas brief odor pulses repeatedly triggered activity in the same coding ensemble, the temporal pattern of synchronous activity superimposed on the ensemble was neither oscillatory nor odor specific. Rather, synchrony strongly depended on contextual variables such as odor intensity and intermittency. Also, because of emergent inhibitory circuit interactions, odor blends evoked temporal ensemble patterns that could not be predicted from the responses to the individual odorants. Thus even at this early stage of information processing, the timing of odor-evoked neural representations is modulated by key stimulus factors unrelated to the molecular identity of the odor.

The insect antennal lobe (AL), a structural and functional analogue of the vertebrate olfactory bulb, receives input from axons of antennal olfactory receptor cells that converge and synapse in discrete modules of condensed neuropil called glomeruli (reviewed in refs. 1, 2). According to a long-standing hypothesis, each glomerulus is functionally unique, and different odorants are represented in the brain by the coordinated activity of different combinations of glomeruli[1,2]. Activity-labeling studies in insects reveal such odor-evoked spatial activity patterns[3–5], but these methods cannot resolve the rapid changes in neuronal firing that underlie odor recognition, and occur on a time scale of milliseconds[6,7]. Similarly, electrophysiological studies show that output or projection neurons (PNs) arborizing in the same glomerulus respond to the same odorant[8], but to date, simultaneous recordings and temporal analysis of spatially distributed glomerular activity are limited to only a few neurons[9,10]. A method that combines the spatial resolution of activity labeling with the temporal resolution of a microelectrode would therefore fill an important gap in helping to decipher the brain's olfactory code. We find that a method originally developed to monitor distributed multi-neuron activity in the mammalian brain[11] can be used to explore the dynamic, spatially organized neural activity patterns evoked by different odors across anatomically and functionally defined glomeruli in the insect olfactory system. Here we show that multi-channel silicon microprobes revealed dynamic, non-linear and unpredictable interactions within ensembles of AL neurons associated with specific, identified olfactory glomeruli[12].

Results

We selected the macroglomerular complex (MGC) in male moths (*Manduca sexta*) for these studies because the MGC is a well characterized array of identified olfactory glomeruli with chemically defined and behaviorally relevant odor input (Fig. 1)[2,8,12]. Experiments in progress confirm that many of the complex odor-evoked neural interactions described here are also observed in non-MGC glomeruli of both male and female moths[13].

Intra- and inter-glomerular neural interactions

In 12 recording sessions lasting at least 3 hours each, we were able to isolate spiking activity from over 50 AL neurons. Up to seven units were separated unambiguously in each experiment, and multi-unit activity was recorded simultaneously from up to eight separate recording sites distributed across a 75×300 µm layer of olfactory neuropil (Fig. 1c). In accord with previous findings, different odors evoked patterns of activity in overlapping yet distinct populations of AL neurons[1–5] (Fig. 1d).

Multi-unit recordings also confirmed the results of our earlier single-neuron intracellular studies, showing that the population of PNs innervating a single glomerulus is physiologically heterogeneous with respect to fine odor tuning[7,8]. Some PNs are narrowly tuned to one odor, whereas the activity of others is modulated by other, often chemically similar odors[12]. Moreover, some PNs are unresponsive to certain stimuli, whereas the ongoing activity of others is suppressed by odor stimulation[14]. This range of complex network interactions is also a prominent feature of mammalian olfactory circuits[15].

In accordance with these findings, examination of odor-evoked ensemble responses revealed that different neurons, although localized to the same glomerulus and responsive to the same odor, were easily discriminated by their unique spike characteristics (Fig. 2a and b). Thus it is possible to identify different subtypes of neurons in ensemble recordings based on specific features of their spike waveforms[10]. We also detected the activities of different physiological subtypes of neurons at the same recording site (Fig. 2b). Although this method does not allow us to determine

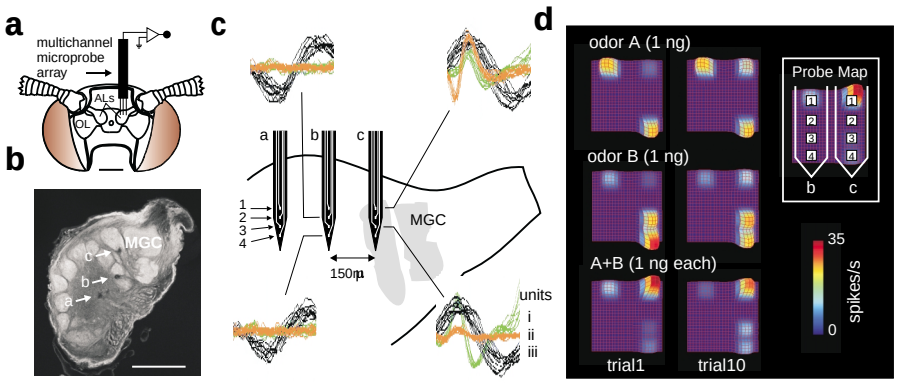

Fig. 1. Ensemble recordings show the dynamics of population responses evoked by odor. (**a**) Experimental set-up and position of the multi-channel probes in one of the antennal lobes (ALs). OL, optic lobe. Scale bar, 1 mm. (**b**) Identification of the positions of the three tracks of a microprobe in the AL, from sections imaged in the confocal microscope (frontal view). The probe tracks were mapped to three locations previously identified in three-dimensional reconstructions of the *M. sexta* AL[17]: track *a* was in the coarse central neuropil, *b* in the array of typical glomeruli, and *c* in the dorsal neuropil of the ring-shaped toroid in the macroglomerular complex (MGC). Scale bar, 250 µm. (**c**) Horizontal reconstruction of probe tracks, and spatial mapping of neural activity to specific recording sites (site separation, 25 µm). Here, spike waveforms from three neurons were clearly discriminated (10–12 superimposed sweeps each), and examples of these spikes recorded simultaneously from tracks *b* and *c* illustrate their isolation to different sites. Only the two neurons recorded from the MGC (green and orange) responded to sex pheromone, reflecting the spatial segregation of different odor signals to different glomeruli. (**d**) Surface plots depicting the spatiotemporal patterns of odor-evoked activity recorded across two probe tracks, both in the MGC. The color scale represents the response magnitudes (maximum instantaneous frequency) of four neurons (three additional neurons were inactive), each localized to a different electrode site. The response to each 100-ms odor pulse was averaged over 100 ms at the response peak. Each odor evoked synchronous activity in different, but overlapping neuron sets, and these patterns were reproducible over repeated trials. Note also that the odor blend (A + B) evoked a strong response from the neuron at site c-1, while simultaneously suppressing activity at all other sites.

the exact origins of these extracellularly recorded signals, it is clear that spikes recorded at one electrode site are not necessarily propagated to another site only 50 µm away (Fig. 1c). Because we have observed clear spatial segregation and differential attenuation of many of these signals across recording sites, we believe that different unit signals detected at the same site reflect the spike activity of different neurons that are in close proximity to that electrode[16]. The recording sites were furthermore localized histologically to specific, identified AL glomeruli[17] (Fig. 1c).

Additionally, unresponsive neurons (for example, neuron 5 in Fig. 2b) were sometimes detected along with responsive neurons at the same recording site. This finding suggests that certain types of neurons may participate in the coding ensemble only in the presence of a particular blend or ratio of odorants[1,2,7,8], or may fire only in other environmental or behavioral contexts (see below).

Neuron-specific firing patterns

Another important feature of these population responses is that the firing patterns of different neurons within the odor-encoding ensemble were specific (Fig. 3). The discharge patterns observed across all neurons in our sample were thus divided into three broadly defined classes: 'fast', 'moderate', and 'diffusely' spiking neurons (Fig. 3). When the firing patterns of different neurons recorded within a 25-µm radius (that is, probably within the same glomerulus) were compared, it was clear that although these neurons responded to the same stimulus, they did not always exhibit the same firing dynamics (Fig. 3). Conversely, neurons recorded at different sites, and responsive to different odors, could display the same firing dynamics (for example, neurons 1 and 2 in Fig. 2). In contrast to findings in mammals[18], these results demonstrate that odor-coding neurons localized to the same glomerulus do not necessarily display the same firing patterns. This is significant because temporal synchronization of firing between neurons with the same discharge pattern could be involved in either intra- or inter-glomerular integration of olfactory information[19]. If functionally related classes of AL neurons synchronize their activity in response to a specific odor blend, for example, this could be an effective mechanism for binding these multiple signal streams into a more coherent representation of the blend stimulus in the brain[19,20].

Temporal binding is context dependent

We tested this hypothesis by computing the extent of synchronous firing across odor-coding AL ensembles (Fig. 4). For exam-

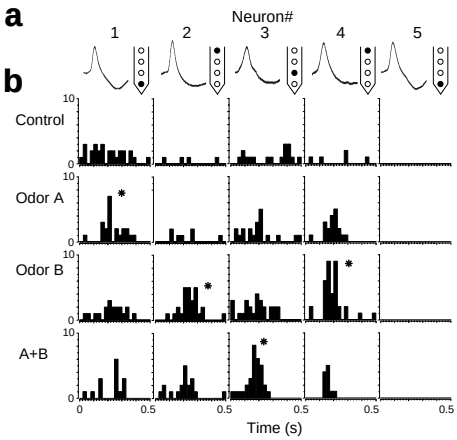

Fig. 2. Simultaneous recordings from multiple neurons show functional differences even among closely spaced cells in the ensemble. (**a**) Average spike waveforms from five neurons discriminated from a single probe track (averages of 126–4,631 events). These are aligned in columns with their odor-evoked responses in (**b**). The position of the recording site yielding the maximum spike amplitude for each neuron is shown next to each waveform in (**a**). Note that spike undershoot was key to distinguishing one neuron from another. (**b**) The five neurons in this ensemble differed in their responses to different odors. Peristimulus histograms show the summed responses to multiple pulses ($n = 20$ for each row) with four different stimuli: air blank (control), 0.1 ng bombykal (odor A), 0.1 ng C15 (odor B), and the blend of the two (A + B). Pulse duration was 100 ms; pulse interval was 1 s (odor onset at time 0). Note that the response profiles of the neurons were strongly heterogeneous, even in this relatively small population. The maximum evoked response (number of spikes per 25-ms bin) for each neuron is indicated by an asterisk.

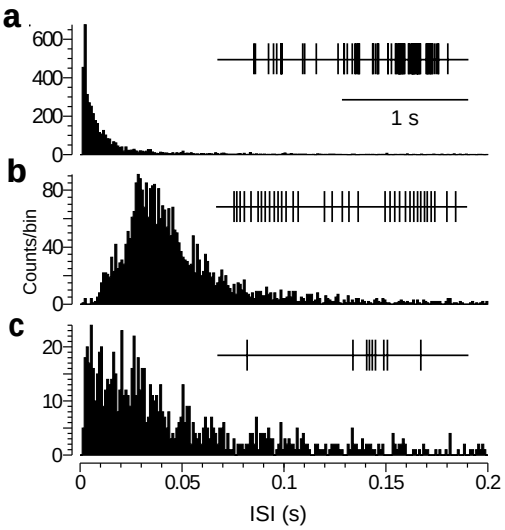

Fig. 3. Different neurons in olfactory glomeruli can be distinguished by their different discharge patterns. Interspike interval (ISI) histograms and rasters (insets) reveal the three distinct temporal patterns of spiking observed across all ensembles: (**a**) 'fast spiking' (sporadic bursts of high-frequency activity); (**b**) 'moderate spiking' (slower, but broader distribution of spike frequencies); (**c**) 'diffuse spiking' (irregular firing). Between 983 and 4,375 events were used to calculate each histogram. These different patterns were frequently visible at the same recording site.

ple, neurons 1 and 2 in Fig. 2 were both classified as moderate spikers and showed a preference for different odors. If the binding hypothesis is correct, we would expect to observe greater coactivity between these neurons when the odor blend is presented than when either of the blend components is presented alone. What we found was surprising: the odor blend indeed resulted in coactivity between neurons 1 and 2, but only when presented at a low dosage (Fig. 4b). At a higher dosage, the blend had the opposite effect: complete desynchronization of spiking activity between the two neurons. Importantly, however, this relationship did not hold for all pairs of cells in the ensemble. Blend-evoked synchronization between neurons 1 and 4, for example, was not apparent at the lower stimulus concentration, but was well developed at the higher dosage (Fig. 4b). The absence of synchronization between these two neurons at the low dosage may have been a consequence of mixture suppression, which was clearly evident in neuron 4. These data therefore provide support for the temporal binding hypothesis, but they also indicate that the expression of binding is a context-dependent phenomenon, contingent on such stimulus variables as concentration (Fig. 4b).

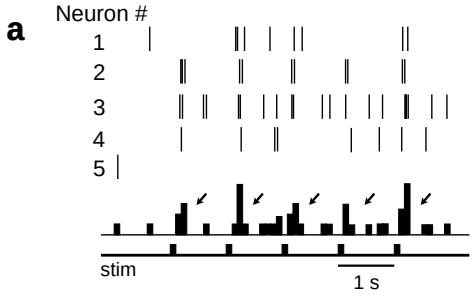

Fig. 4. Odor blends evoked network dynamics that could not be predicted from the responses to the individual odors in the blend. (**a**) Responses from the five-neuron ensemble (**Fig. 2**) are shown as rasters. Five 100-ms odor-blend pulses were delivered at 1 Hz to simulate naturally brief and intermittent stimulus conditions (stim). Peri-event histogram (below rasters) illustrates how the overall activity of the ensemble is time-locked to the stimulus pulses. Note, however, that some neurons (such as #2) were more tightly stimulus-locked than others. Each odor pulse evoked a discrete burst of spikes across the population, followed immediately by strong suppression (arrows) that helped to further synchronize the population response to the stimulus. (**b**) The complex patterns of neuronal synchrony evoked by two different odors (A, B) and their blend (A+B) at two dosages are represented as color-coded coactivity matrices. The number of synchronous events (10- or 15-ms window; **Fig. 5**) evoked by each odor pulse was calculated for 0.5 s from stimulus onset, and averaged over 20 trials (color scale ranges from 0–3.8 coincident spikes per stimulus; two-way repeated measures ANOVA; $F = 18.28$, $p < 0.005$). The horizontal display beneath each matrix shows the mean firing rate for each neuron individually (color scale ranges from 0–5.5 spikes per stimulus; $F = 13.79$, $p < 0.005$). Responses over 20 consecutive trials showed neither significant changes in intensity with time ($F = 1.54$, $p > 0.1$) nor significant changes in synchrony with time ($F = 1.47$, $p > 0.1$), in contrast to results reported in the locust AL[27].

Further examination of ensemble patterns yielded clear evidence for complex and multiple blend effects within a single odor-encoding assembly. When compared to the responses evoked by odor B alone, the low-dosage odor blend evoked significantly greater firing rates in neurons 2 and 3, whereas a significant blend-induced suppression of activity was observed in neuron 4 (first column in Fig. 4b). This odor blend also led to increased coactivity in some neuron pairs (neurons 1 and 2, 2 and 3, 2 and 4), leaving the other pairs completely desynchronized. The higher-dosage odor blend also led to increased coactivity between neurons 2 and 3, but unlike

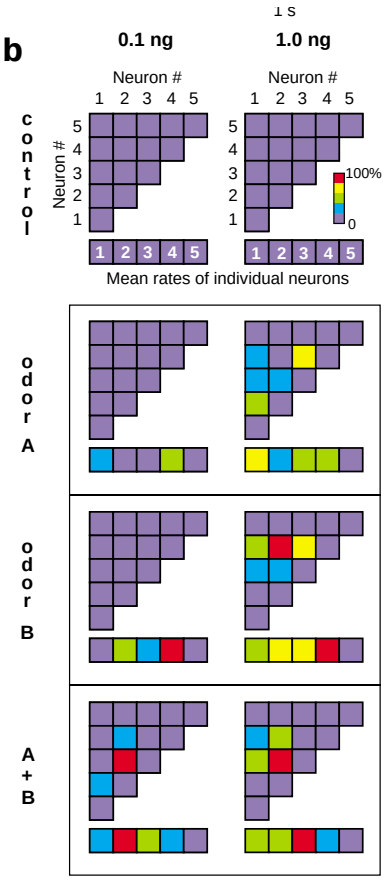

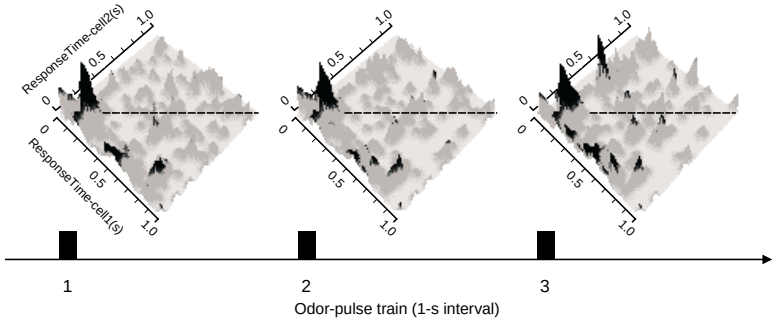

Fig. 5. Time course of odor-evoked coactivity within the ensemble. Dynamic correlation analysis revealed that the temporal structure of the ensemble response was modulated by stimulus dynamics. Each surface plot shows how the cross correlations between two neurons changed as a function of time. The odor stimulus (odor B, 1 ng) was presented at time 0 in each panel, and both neurons responded to repeated stimulus pulses after an expected latency. (Only three stimulus–response epochs are shown here for detail.) An incidence of high correlation (spikes in the two neurons synchronized to within 15 ms) is shown as a prominent peak along the diagonal (indicated by the dashed line). Although there is some variability in the time course of the response from trial to trial, note how the period of maximum coactivity in each correlogram is time-locked to the stimulus pulse. This peak furthermore is followed consistently by a period of suppression and spike desynchronization until the next stimulus pulse. Note also the absence of any regular periodicity in the responses to these brief, 100-ms odor pulses.

the lower-dosage blend, it also enhanced synchrony between neurons 1 and 3 (second column in Fig. 4b). At the same time, the higher-dosage blend resulted in a significant reduction in synchrony between other pairs (neurons 1 and 2, 2 and 4, 3 and 4).

Finally, we wanted to know whether the patterns of synchrony we observed were governed by oscillatory network dynamics, as in other invertebrate and vertebrate olfactory systems (reviewed in ref. 21), or whether coactivity among neurons in an ensemble is linked to other factors. We examined the spike trains from 17 pairs of AL neurons (tentatively identified as PNs) for evidence of an underlying oscillation. Dynamic cross-correlation analysis revealed that brief odor pulses consistently failed to evoke rhythmic spike discharge in single neurons, and furthermore failed to evoke a rhythmic pattern of coactivity between neurons (Fig. 5). Instead, odor-responsive neurons were coactive only during a brief time window following the stimulus, and this transient synchrony was followed by a pronounced period of suppression and return to baseline activity until the next odor pulse (Fig. 5). These results collectively show that the formation of patterned odor representations in these glomerular networks involves both excitatory and inhibitory cellular interactions, and that the temporal structure of these ensemble responses is neither oscillatory nor stimulus specific, but strongly context dependent.

Discussion

The application of ensemble recording methods to the analysis of olfactory-system function opens up many possible avenues for testing established hypotheses about the functional roles of olfactory glomeruli in odor recognition and discrimination. Ensemble data add a necessary dimension to the analysis of the complex intercellular relationships that emerge when glomerular circuits in the olfactory system process information under naturalistic conditions, when stimulus presentation is intermittent and unpredictable[22]. In addition, this recording strategy enables us to explore central coding of odor information in another important context—learning. Behavioral studies using *M. sexta*, modeled after proboscis-extension training in honeybees[23], show that moths can learn (even after a single trial) to associate an odor stimulus with a food reward[24,25]. By combining behavioral conditioning with chronic ensemble recording, we now can monitor odor-evoked ensemble activity before, during and after olfactory reinforcement training, and compare these responses over time in the same animal. (K.C. Daly, T.A.C., V.M.P., B.H. Smith & J.G.H., *Assoc. Chemoreception Sci. Abstr.* 35, 2000.) This approach will be used to probe how olfactory experience affects odor coding in the brain, and will facilitate the analysis of neural interactions underlying the acquisition, retention and extinction of these learned associations.

Odor-modulated oscillatory dynamics are a prominent feature of numerous olfactory systems, including that of *M. sexta*[26], and olfactory information processing in both vertebrates and invertebrates is thought to involve oscillatory synchronization of ensemble activity[9,20,21,27]. However, whether different odors are each encoded by a unique oscillatory pattern of ensemble activity remains controversial, because most studies have not addressed how the brain discriminates one odor from another when the stimulus is sufficiently brief and/or intermittent that network oscillations are unable to develop[22]. Using brief, intermittent odor pulses in the present study, we find that the temporal patterning of odor-evoked ensemble responses is consistent with our previous single-neuron data: that is, the firing patterns of glomerular PNs depend not only on the chemistry of the odor but also on the physical context in which the odor is delivered[22]. Our new data also show that, because of emergent properties of glomerular networks, the patterns of synchrony among different members of an odor-encoding ensemble are not the same for different concentrations of the same odor. Furthermore, the responses to odor blends cannot necessarily be predicted from the responses to the individual odors in the blend. We therefore propose that ensembles of olfactory PNs must use multiple and overlapping coding strategies to process olfactory information, and that these strategies are matched to the particular circumstances surrounding odor presentation. Through their complex spiking patterns, they must report primary information about both the chemical identity of the stimulus (through their specific spatial association with one or more glomeruli), as well as information regarding stimulus intensity and the spatiotemporal distribution of odor in space (information that is ecologically relevant to locating the odor source)[22] . Our results also suggest that in some stimulus contexts, oscillations are not necessary for synchronizing odor-encoding neural ensembles at the first stage of glomerular processing. For animals that must continually monitor changes in a dynamic odor plume, a lack of dependence on oscillations is advantageous—the necessary information about stimulus dynamics could be easily corrupted or lost completely if an underlying periodicity were to modulate the network response to odor.

Methods

Preparation. *Manduca sexta* (L.; Lepidoptera, Sphingidae) were reared on an artificial diet under a long-day (14L:10D) photoperiod. Adult moths, one to four days after emergence, were used in all experiments. In preparation for recording, the moth was restrained in a plastic tube with its head and antennae fully exposed. The labial palps, proboscis and cibarial musculature were then removed to allow frontal access to the

brain[7]. The head was secured to the plastic tube with wax, and then the tube was fixed to the recording table and situated with the ALs facing upward. The tracheae overlying one AL were then removed with fine forceps. The brain was superfused slowly with physiological saline solution (150 mM NaCl, 3 mM $CaCl_2$, 3 mM KCl, 10 mM TES buffer and 25 mM sucrose, pH 6.9) for the duration of the experiment.

Ensemble recording and data analysis. To study population responses across glomeruli, we used multi-channel silicon microprobe arrays, supplied by the University of Michigan's Center for Neural Communication Technology. We selected a probe design that matched the spatial dimensions of the MGC in the AL of male *M. sexta* (Fig. 1). Fork-like probes with three tines, with four recording sites per tine (eight were active) were inserted into the MGC and other glomeruli using several key landmarks. The final depth of the probes was noted, and the exact locations of the three tines and their recording sites were verified histologically (Fig. 1b). Recording sites measured 9×12 µm, and were separated by 25 µm; thus multiple sites could be situated in a single glomerulus.

Multi-neuron activity was recorded simultaneously on eight channels (Lynx-8 amplifier, Neuralynx, Tucson, Arizona). Spike data were extracted from the recorded signals and digitized at 20 kHz per channel using Data Wave's Discovery acquisition software and Data Translation's 2821-G 16SE A/D board on a Pentium III platform (Data Wave Technologies, Longmont, Colorado). Filter settings (typically 0.6–3 kHz) and system gains (typically 5–20 K) were software-adjustable on each channel. Multiple spike waveform parameters were extracted and used to classify different units based on multi-dimensional cluster analysis. Only those spike clusters that were verified statistically by multivariate discriminant analysis (Wilks' lambda test) were used for further analysis. Each spike in each separated cluster was time stamped, and these data were used to calculate peristimulus histograms, inter-spike interval histograms, mean-rate values, and the number of nearly coincident firings between all neurons in each ensemble (NeuroExplorer, Nex Technologies, Winston-Salem, North Carolina). All data were normalized to correct for components of the correlation caused directly by modulation of the stimulus[28].

Odor stimulation. The solenoid-driven device for odor delivery has been described[7,10,12]. For most trials, several stimulus patterns were presented to the antenna: a single, 200-ms odor pulse was the most common stimulus, but 5–20 sequential 50 or 100-ms pulses were also presented to examine changes over repeated trials. The odorants used are the two essential components of the sex pheromone of *M. sexta*, bombykal (E10,Z12-hexadecadienal; odor A) and E11,Z13-pentadecadienal ('C15', a mimic of the second key component, E10,E12,Z14-hexadecadienal; odor B)[12], as well as binary blends of the two.

Histological identification of recording sites. Immediately following a recording session, the brain was excised and immersed in 1–2% glutaraldehyde in 0.1 M phosphate buffer to increase contrast. Brains were fixed for at least one hour, then dehydrated by passage through a graded ethanol series, and finally embedded in Spurr's resin (Electron Microscopy Sciences, Ft. Washington, Pennsylvania) in preparation for serial sectioning. Sections were cut at 48 µm on a sliding microtome, and 2-µm optical sections were collected with a laser-scanning confocal microscope (Bio-Rad MRC-600, Cambridge, Massachusetts, equipped with a Nikon Optiphot-2 microscope). This method reliably revealed the location of each of the three tines of the silicon microprobes in the AL without the need for tissue staining (Fig. 1b).

Acknowledgements

We are grateful to David Anderson and coworkers for providing microprobes and technical support, and we thank Carol Barnes and Bruce McNaughton for advice. We also thank Kevin Daly and Brian Smith for discussions and comments, and Heather Stein and A.A. Osman for technical assistance. Supported by grants and contracts from NIH/NIDCD and DARPA/CBS.

Received 18 April; Accepted 17 July 2000

1. Hildebrand, J. G. & Shepherd, G. M. Mechanisms of olfactory discrimination: converging evidence for common principles across phyla. *Annu. Rev. Neurosci.* 20, 595–631 (1997).
2. Christensen, T. A. & White, J. in *The Neurobiology of Taste and Smell* Vol. 2 (eds. Finger, T. E., Silver, W. L. & Restrepo, D.) (Wiley, New York, in press).
3. Rodrigues, V. Spatial coding of olfactory information in the antennal lobe of Drosophila melanogaster. *Brain Res.* 453, 299–307 (1988).
4. Joerges, J., Küttner, A., Galizia, G. & Menzel, R. Representations of odours and odour mixtures visualized in the honeybee brain. *Nature* 387, 285–288 (1997).
5. Distler, P. G., Bausenwein, B. & Boeckh, J. Localization of odor-induced neural activity in the antennal lobes of the blowfly Calliphora vicina: a [3H]2-deoxyglucose labeling study. *Brain Res.* 805, 263–266 (1998).
6. Murlis, J. in *Insect Pheromone Research – New Directions* (eds. Carde, R. T. & Minks, A. K.) 221–231 (Chapman & Hall, New York, 1997).
7. Christensen, T. A. & Hildebrand, J. G. Coincident stimulation with pheromone components improves temporal pattern resolution in central olfactory neurons. *J. Neurophysiol.* 77, 775–781 (1997).
8. Hansson, B. S. & Christensen, T. A. in *Insect Olfaction* (ed. Hansson, B. S.) 125–161 (Springer, Berlin, 1999).
9. Stopfer, M., Wehr, M., MacLeod, K. & Laurent, G. in *Insect Olfaction* (ed. Hansson, B. S.) 163–180 (Springer, Berlin, 1999).
10. Christensen, T. A., Waldrop, B. R., Harrow, I. D. & Hildebrand, J. G. Local interneurons and information processing in the olfactory glomeruli of the moth *Manduca sexta*. *J. Comp. Physiol. A* 173, 385–399 (1993).
11. Nicolelis, M. A. L. *Methods for Neural Ensemble Recordings* (CRC, New York, 1999).
12. Heinbockel, T., Christensen, T. A. & Hildebrand, J. G. Temporal tuning of odor responses in pheromone-sensitive projection neurons in the brain of the sphinx moth *Manduca sexta*. *J. Comp. Neurol.* 409, 1–12 (1999).
13. King, J. R., Christensen, T. A. & Hildebrand, J. G. Response characteristics of an identified, sexually dimorphic olfactory glomerulus. *J. Neurosci.* 20, 2391–2399 (2000).
14. Christensen, T. A. & Hildebrand, J. G. Male-specific, sex pheromone-selective projection neurons in the antennal lobes of the moth Manduca sexta. *J. Comp. Physiol. A* 160, 553–569 (1987).
15. Mori, K. & Shepherd, G. M. Emerging principles of molecular signal processing by mitral/tufted cells in the olfactory bulb. *Seminars Cell Biol.* 5, 65–74 (1994).
16. Buonviso, N. & Chaput, M. A. Response similarity to odors in olfactory bulb output cells presumed to be connected to the same glomerulus: electrophysiological study using simultaneous single-unit recordings. *J. Neurophysiol.* 63, 447–454 (1990).
17. Rospars, J. P & Hildebrand, J. G. Anatomical identification of glomeruli in the antennal lobes of the male moth *Manduca sexta*. *Cell Tissue Res.* 270, 205–227 (1992).
18. Buonviso, N., Chaput, M. A. & Berthommer, F. Temporal pattern analyses in pairs of neighboring mitral cells. *J. Neurophysiol.* 68, 417–424 (1992).
19. Rieke, F., Warland, D., de Ruyter van Steveninck & Bialek, W. *Spikes: Exploring the Neural Code* (MIT Press, Cambridge, Massachusetts, 1997).
20. Kashiwadani, H., Sasaki, Y. F., Uchida, N. & Mori, K. Synchronized oscillatory discharges of mitral/tufted cells with different molecular receptive ranges in the rabbit olfactory bulb. *J. Neurophysiol.* 82, 1786–1792 (1999).
21. Gelperin, A. Oscillatory dynamics and information processing in olfactory systems. *J. Exp. Biol.* 202, 1855–1864 (1999).
22. Christensen, T. A., Waldrop, B. R. & Hildebrand, J. G. Multitasking in the olfactory system: context-dependent responses to odors reveal dual GABA-regulated coding mechanisms in single olfactory projection neurons. *J. Neurosci.* 18, 5999–6008 (1998).
23. Faber, T., Joerges, J. & Menzel, R. Associative learning modifies neural representations of odors in the insect brain. *Nat. Neurosci.* 2, 74–78 (1999).
24. Daly, K. C. & Smith, B. H. Associative olfactory learning in the moth *Manduca sexta*. *J. Exp. Biol.* (in press).
25. Hartlieb, E. Olfactory conditioning in the moth *Heliothis virescens*. *Naturwissenschaften* 83, 87–88 (1996).
26. Heinbockel, T., Kloppenburg, P. & Hildebrand, J. G. Pheromone-evoked potentials and oscillations in the antennal lobes of the sphinx moth *Manduca sexta*. *J. Comp. Physiol.* A. 182, 703–714 (1998).
27. Stopfer, M. & Laurent G. Short-term memory in olfactory network dynamics. *Nature* 402, 664–668 (1999).
28. Aertsen, A. M. H. J., Gerstein, G. L., Habib, M. K. & Palm, G. Dynamics of neuronal firing correlation: modulation of "effective connectivity". *J. Neurophysiol.* 61, 900–917 (1989).